The Possible Role of SO_3 as an Oxidizing Agent in Methane Functionalization by the Catalytica Process. A Density Functional Theory Study

Iordan H. Hristov[†] and Tom Ziegler*[,‡]

Department of Chemistry, University of Calgary, 2500 University Drive NW, Calgary, Alberta, Canada T2N 1N4

Received September 17, 2002

The Catalytica process converts methane to methyl bisulfate in good yield at relatively low temperature in fuming sulfuric acid with (bipyrimidine)$PtCl_2$ as a catalyst. Previously we examined the first step, methane C−H activation, and here we look at the oxidation by SO_3 and the reductive elimination steps. In the oxidation step a Pt(II)−CH_3 complex (**a**) reacts with protonated SO_3, which splits to form two new ligands, SO_2 and OH^-, thus oxidizing **a** to a Pt(IV)−CH_3 complex. The final step in the cycle is the reductive elimination of methyl bisulfate from this complex.

Introduction

Methane is the major constituent of natural gas, which is an abundant and inexpensive natural resource. Currently its high transportation cost and low reactivity prevent it from being used fully as a major feedstock for the chemical industry. In the existing technology methane is transformed to syngas (CO + H_2) at high temperature and pressure, which can be converted further to methanol. A low-temperature method for the direct oxidation of methane would be an attractive alternative. The major problem with oxidation is the selectivity of the process: the desired products are more reactive than methane itself and are oxidized to CO_2.

It has been known since the early 1970s that Pt(II) can activate C−H bonds in methane. Further, Pt(IV) has been shown to oxidize methane to methanol.[1] This represents one of the first homogeneous processes for methane oxidation in which the product (methanol) was very stable toward further oxidation. The oxidizing agent, Pt(IV), however is impractical for any industrial applications. In the Catalytica process[2] the oxidation of methane is achieved by SO_3 in fuming sulfuric acid at 220 °C. The catalyst is (bpym)$PtCl_2$, which has the desired activity for methane activation and is stable under the reaction conditions. The product is methyl bisulfate, which can readily be hydrolyzed. The selectivity that was achieved based on methane was 81% with a one-pass yield of 72%. The SO_2 byproduct is also readily oxidized to SO_3, thus providing a plausible catalytic cycle.

The mechanism (Scheme 1) that was proposed for the Catalytica process is based on Shilov's C−H activation reactions ($[PtCl_4]^{2-}$/$[PtCl_6]^{2-}$ in aqueous acetic acid).[1] It includes the following steps: formation of a 14-electron cationic Pt(II) complex (**B**), which reacts with methane to form a Pt(II)−methyl complex (**C**); oxidation of **C** to a Pt(IV)−CH_3 complex; reductive elimination of methyl bisulfate and loss of a bisulfate ligand to regenerate the catalyst **B** (Scheme 1).

Scheme 1. Proposed Mechanism for the Catalytica Process

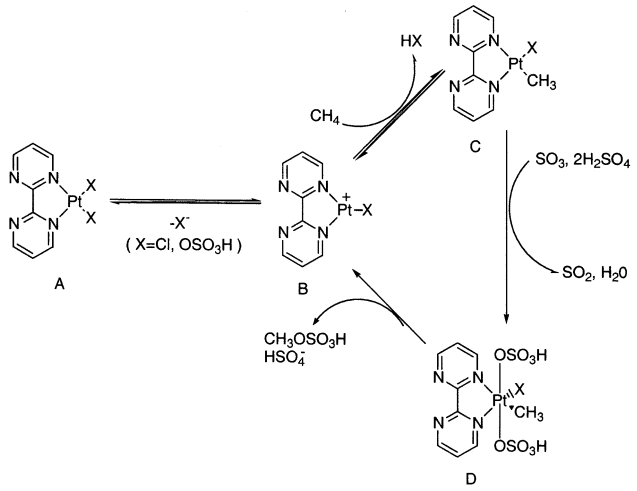

Previously we examined[3] the activation step, looking into two possible mechanisms, oxidative addition and metathesis (Figure 1). In the present investigation we shall concentrate on the remaining steps in the cycle given in Scheme 1.

The process of methane activation by Pt(II) complexes has been examined before in a number of theoretical studies.[4]

[†] E-mail: hristov@ucalgary.ca.
[‡] E-mail: ziegler@ucalgary.ca. Fax: (403) 289-9488.

(1) Gol'dshleger, N. F.; Es'kova, V. V.; Shilov A. E.; Shteinman, A. A. *Zh. Fiz. Khim.* (Engl. Transl.) **1972**, *46*, 785.
(2) Periana, R. A.; Taube, D. J.; Gamble, S.; Taube, H.; Satoh, T.; Fujii, H. *Science* **1998**, *280*, 560.
(3) Gilbert, T. M.; Hristov, I. H.; Ziegler, T. *Organometallics* **2001**, *20(6)*, 1183.
(4) (a) Mylvaganam, K.; Backskay, G. B.; Hush, N. S. *J. Am. Chem. Soc.* **1999**, *121* (19), 4633. (b) Barlett, K. L.; Goldberg, K. I.; Borden, W. T. *J. Am. Chem. Soc.* **2000**, *122* (7), 1456. (c) Mylvaganam, K.; Backskay, G. B.; Hush, N. S. *J. Am. Chem. Soc.* **2000**, *122* (9), 2041. (d) Mylvaganam, K.; Backskay, G. B.; Hush, N. S. *J. Am. Chem. Soc.* **1999**, *121* (19), 4633.

10.1021/om020774j CCC: $25.00
Publication on Web 03/19/2003

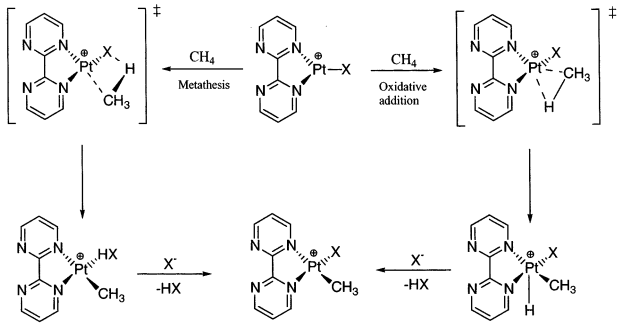

Figure 1. Transition states in the C−H activation. In the metathesis the C−H stretching is in the plane of the complex, while in the oxidative addition it is normal to the complex.

Computational Details

All DFT calculations were carried out using the Amsterdam Density Functional (ADF 2.3.3) program[5a] developed by Baerends et al.[5b] and vectorized by Ravenek.[5c] The numerical integration scheme applied for the calculations was developed by te Velde et al.[5d,e] The geometry optimization procedure was based on the method of Versluis and Ziegler.[5f] Geometry optimizations were carried out and energy differences determined using the local density approximation of Vosko, Wilk, and Nusair (LDA VWN)[5g] augumented with the nonlocal gradient correction PW91 from Perdew and Wang.[5h] Relativistic corrections were added using a scalar-relativistic Pauli Hamiltonian.[5i] The electronic configurations of the molecular systems were described by a triple-ζ basis set for all atoms. Non-hydrogen atoms were assigned a relativistic frozen-core potential, treating as core shells up to and including 4f for Pt, 2p for Cl and S, and 1s for C, N, and O. A set of auxiliary s, p, d, and f functions, centered on all nuclei, was used to fit the molecular density and to represent the Coulomb and exchange potentials accurately in each SCF cycle. Transition states were located from a linear transit scan in which the reaction coordinate was kept fixed at different distances while all other degrees of freedom were optimized. Solvation energies were calculated from gas phase structures by using the Conductor-like Screening Model (COSMO)[5j] that has been recently implemented into the ADF program.[5k] The solvation calculations were performed with a dielectric constant of 100 for sulfuric acid. The radii used for the atoms (in Å) are as follows: H, 1.16; S, 1.7; C, 2.3; O, 1.3; Cl, 1.8; N, 1.4; Pt, 1.387. These values were obtained by optimization using least-squares fitting to experimental solvation energies.[5l] Detailed structural data are available as Supporting Information.

Results and Discussion

The main objective of our investigation involves the oxidation of Pt(II) by SO_3. However we shall first clarify a few points left over from our study of the C−H activation step. The first point concerns what happens to the catalyst (bpym)$PtCl_2$ in sulfuric acid. It is possible that the bipyrimidine ligand undergoes protonation by one or two H^+ units to form cationic species. Further, the chloride ligands could be exchanged with bisulfate. In the case of ammonia ligands the protonation was observed by Periana and led to dissociation of NH^+_4 and loss of catalyst activity. In our case however we were surprised that the bipyrimidine ligand was not protonated. The first protonation of eq 1 was calculated to be endothermic by 6.9 kcal/mol, whereas the second protonation of eq 2 was endothermic by 17.5 kcal/mol in solution.

$$(\text{bpym})PtCl_2 + H_2SO_4 \rightarrow (\text{bpymH})PtCl_2^+ + HSO_4^- \quad (1)$$

$$(\text{bpymH})PtCl_2^+ + H_2SO_4 \rightarrow (\text{bpym(H)}_2)PtCl_2^{2+} + HSO_4^- \quad (2)$$

However monoprotonation of bipyrimidine itself is favorable by −5.5 kcal/mol.

Another possible transformation of (bpym)$PtCl_2$ in sulfuric acid involves the substitution of one or two Cl^- ligands by HSO_4^- groups.

$$(\text{bpym})PtCl_2 + H_2SO_4 \rightarrow (\text{bpym})PtHSO_4Cl + HCl \quad (3)$$

$$(\text{bpym})PtHSO_4Cl + H_2SO_4 \rightarrow (\text{bpym})Pt(HSO_4)_2 + HCl \quad (4)$$

We calculated the heat of reaction of the first process in oleum to be $\Delta H_3 = 15.4$ kcal/mol. The corresponding calculated value for the second process was $\Delta H_4 = 14.7$ kcal/mol. We cannot conclusively estimate the enthalpies in reactions 1 through 4 due to the simple solvation model used. However we shall in the following consider (bpym)$PtCl_2$ as the active catalyst.

In our previous study on methane activation by (bpym)$PtCl_2$ it was assumed that Cl^- would dissociate to form the tricoordinate species **B** followed by activation of methane. The energy required to form **B** is 47 kcal/mol. An alternative path would be the nucleophilic displacement of Cl^- by methane from (bpym)$PtCl_2$. The estimated barrier is 38.9 kcal/mol in solution, and the transition state is shown in Figure 2a.

In the transition state of this exchange reaction both the methane and the chloride ligands are very far from the metal center. The Pt−Cl bond is stretched from 2.29 Å to 3.98 Å, and the Pt−CH_4 bond is at 2.78 Å. In the case of bisulfate ligand displacement the barrier is 33.1 kcal/mol in solution. The transition state structure (Figure 2b) shows the formation of the Pt−CH_4 bond with a bond length of 2.51 Å, while the Pt−bisulfate bond length is stretched from 2.03 Å to 2.81 Å. The stronger Pt−methane interaction here can be attributed to the greater electronegativity of the bisulfate ligand, which makes the metal center more electrophilic. Thus, although chloride is the preferred ligand in the coordination sphere of platinum, bisulfate provides for a lower energy barrier in the ligand exchange reaction.

(5) (a) *Amsterdam Density Functional program*; Division of Theoretical Chemistry, Vrije Universiteit: De Boelelaan 1083, 1081 HV Amsterdam, The Netherlands; www.scm.com. (b) Baerends, E. J.; Ellis, D. E.; Ros, P. *Chem. Phys.* **1973**, *2*, 41 and 52. (c) Ravenek, W. In Algorithms and *Applications on Vector and Parallel Computers*; te Riele, H. J. J., Dekker, T. J., van de Horst, H. A., Eds; Elsevier: Amsterdam, The Netherlands, 1987. (d) Boerrigter, P. M.; te Velde, G.; Baerends, E. J. *J. Comput. Chem.* **1988**, *33*, 87. te Velde, G.; Baerends, E. J. *J. Comput. Chem.* **1992**, *99*, 84. (e) te Velde, G.; Baerends, E. J. *J. Comput. Chem.* **1992**, *99*, 84. (f) Versluis, L.; Ziegler, T. *J. Chem. Phys.* **1988**, *88*, 322. (g) Vosko, S. H.; Wilk, L.; Nusair, M. *Can. J. Phys.* **1980**, *58*, 1200. (h) Perdew, J. P.; Chevary, J. A.; Vosko, S. H.; Jackson, K. A.; Pederson, M. R.; Singh, D. J.; Fiolhais, C. *Phys. Rev. B* **1992**, *46*, 6671. (i) Sinjders, J. G.; Baerends, E. J.; Ros, P. *Mol. Phys.* **1979**, *38*, 1909. (j) Klamt, A.; Schuurmann, G. *J. Chem. Soc., Perkin Trans.* **1993**, *2*, 799. (k) Rye, C. C.; Ziegler, T. *Theor. Chem. Acc.* **1999**, *101*, 396. (l) Marcus, Y. *J. Chem. Soc., Faraday Trans.* **1991**, *87* (18), 2995.

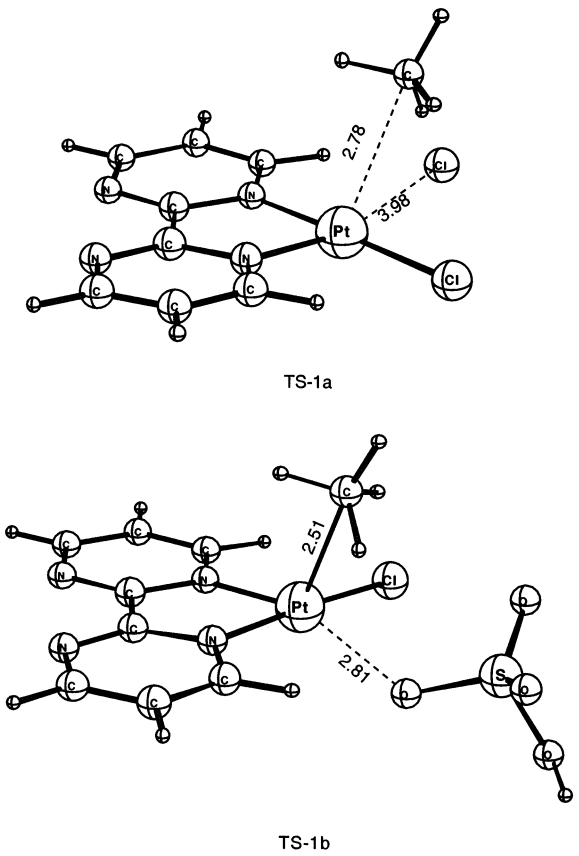

Figure 2. Transition states for the ligand exchange reactions for (a) (bpym)$PtCl_2$ and (b) (bpym)$PtCl(HSO_4)$. The structures were found with a constrained optimization in solution.

The C−H activation of methane in (bpym)$Pt(CH_4)$-Cl^+ proceeds most favorably through an oxidative addition mechanism with a barrier of 10 kcal/mol in solution, whereas (bpym)$Pt(CH_4)HSO_4^+$ prefers the metathesis mechanism with a barrier of 8.9 kcal/mol.[3] This can be explained by the higher electronegativity of the bisulfate, which makes an oxidative addition at the more electron poor center harder compared to the chloride case. The overall heat of reaction 5 is $\Delta H_5 =$ 24.2 kcal/mol in solution.

$$(\text{bpym})PtCl_2 + CH_4 \rightarrow (\text{bpym})PtCH_3Cl + HCl \quad (5)$$

Oxidation. The next step in the Catalytica cycle is the oxidation of complex **C** (Scheme 1) by SO_3. Alternatively **A** of Scheme 1 could be oxidized and the product could in turn oxidize **C**. This would be equivalent to the oxidation in the Shilov system,[1] where the oxidizing agent is $[PtCl_6]^{2-}$. The oxidation in the Shilov system proceeds by an inner-sphere, two-electron transfer from $(CH_3)Pt(II)$ to Pt(IV) (i.e., chloronium ion transfer). We have for this reason looked at the oxidation of **A** by SO_3 as an alternative way in which to produce Pt(IV) species that can subsequently oxidize $(CH_3)Pt(II)$.

The mechanism we propose for the oxidation of **A** and **C** by SO_3 is the following (Figure 3): (a) association of SO_3 to the Pt(II) complex (1 → 2), (b) protonation of one of the oxygens on SO_3 (2 → 3), (c) stretching of the S−OH bond mediated by Pt to form a new OH ligand (3 → 4 → 5), (d) dissociation of SO_2 (5 → 6), (e) abstraction of OH^- and addition of HSO_4^- (6 → 7). The energies along the reaction path for the oxidation of (bpym)$PtCl_2$ and (bpym)$Pt(CH_3)Cl$ in solution can be seen in Scheme 2.

The energetics for the oxidation of the two complexes exhibit a number of differences. The SO_3 adduct for the methyl complex is more stable by 6.91 kcal/mol, and the Pt−S bond length of the methyl complex with R(Pt−S) = 2.61 Å is 0.25 Å shorter than the corresponding bond length in the dichloro complex with R(Pt−S) = 2.86 Å. The protonation at the SO_3 oxygen leads to a dramatic difference: destabilization of the dichloro complex by 9.2 kcal/mol compared to only 0.4 kcal/mol for the methyl complex. The geometries are however similar: R(Pt−S) = 2.39 Å for the dichloro system and 2.35 Å for the methyl complex. To explain these differences and to get more insight into the oxidation processes, we carried out a fragment orbital population analysis for the SO_3 and the protonated SO_3 aducts (compounds 3) in gas phase in terms of the molecular orbitals of SO_3 and SO_3H^+ as well as the complexes **A** and **C** of Scheme 1. Our fragment analysis of the adducts revealed that the main bonding interaction involves the LUMO orbitals of SO_3 and SO_3H^+ as well as the occupied d_{z^2} orbital of the platinum complex. This interaction changes the geometry of the SO_3 and SO_3H^+ species, from a planar conformation in the free fragments to a trigonal pyramidal conformation in the adduct complex, where the sulfur atom extends below the plane of the oxygens. The change of the shape of the LUMO orbitals and their energies is substantial, as SO_3 and SO_3H^+ are distorted from planarity.

In the case of SO_3 the LUMO of the free fragment is at −3.975 eV, whereas the LUMO energies of the distorted SO_3 fragments are at −5.098 and −6.476 eV for the dichloro and methyl complexes, respectively. The SO_3 fragments have different geometries in the two adducts, and thus different LUMO energies. The SO_3 fragment in the methyl adduct deviates most from planarity, and the corresponding LUMO has, as it will become evident shortly, the lower energy. The change in the structure of SO_3 on complexation is shown in Figure 4.

The free SO_3 species has its LUMO formed from the 2p orbitals of oxygen lying in the plane of the molecule, separated by two negative lobes on the sulfur, normal to the plane. The sulfur orbital is a s−d_{z^2} hybrid combination that is seen to interact in an antibonding fashion with the 2p oxygen orbitals. The SO_3 species forming adducts with complexes **A** and **C** of Scheme 1 are pyramidal, which changes the constitution of the LUMO orbitals, as evident in Figure 4b. Here we have the 2p orbitals of oxygen normal to the plane, and the sulfur has only a positive lobe made up of an s−p hybrid orbital. There is only a small antibonding interaction in these LUMOs because the sulfur is below the plane of the oxygens. The donor orbital on the metal fragments is the d_{z^2} orbital of Pt. Its energy is −5.968 eV for Pt-(II)−CH_3 and −6.476 eV for Pt(II)−Cl. The formation of the adduct with Pt(II)−CH_3 is more favorable because the donating orbital is higher in energy. The SO_3 fragment accepts electron density from Pt, building a negative charge of 0.22 and 0.38 in the dichloro and methyl complexes, respectively. The larger donation of

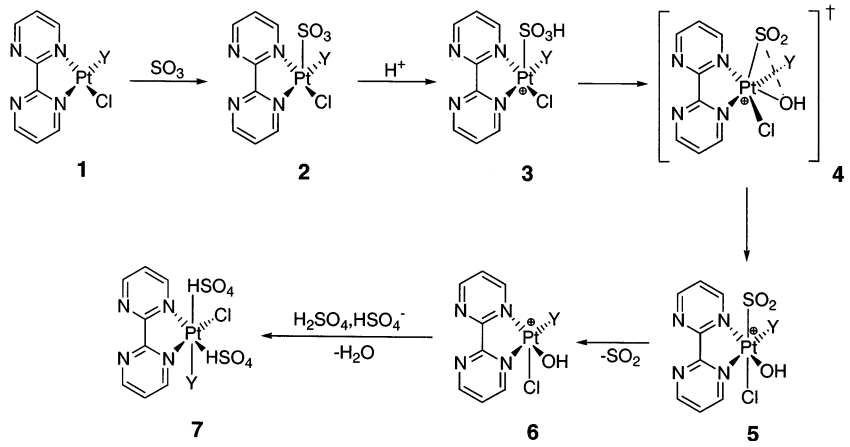

Figure 3. Proposed mechanism for the oxidation of the Pt(II)−Y complexes Y=Cl or CH_3.

Scheme 2. Energy Profile for the Oxidation Mechanism[a]

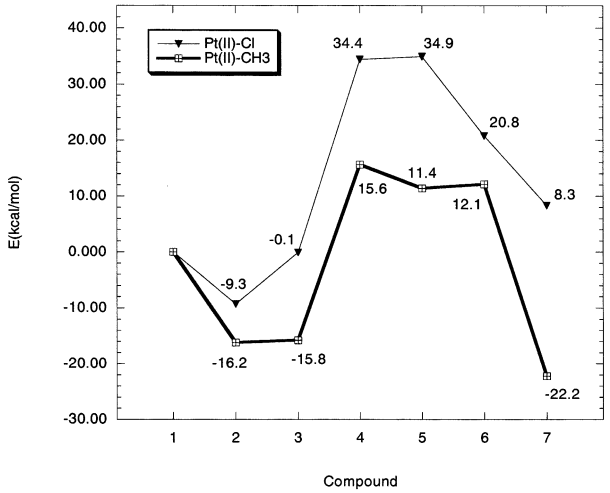

[a] Energies are in kcal/mol in solution. Solid line: (bpym)-$PtCH_3Cl$. Hairline: (bpym)$PtCl_2$. The compounds are from Figure 3.

Figure 4. LUMO orbitals of SO_3.

electron charge to SO_3 in the methyl complex causes the SO_3 fragment in this case to be more pyramidal.

In the case of SO_3H^+ the LUMO of the free fragment is at −11.569 eV, whereas for the dichloro and methyl complexes the LUMO of the SO_3H^+ fragment is −14.155 and −14.274 eV, respectively. The change in the structure of SO_3H^+ upon association with the Pt(II) complex is shown in Figure 5.

The shape of the LUMO orbital for SO_3H^+ has some similarity to that of SO_3. The free fragment's sulfur orbital is again an s−d hybrid (although here the dominating d orbital is x^2-y^2). The LUMO of the associated SO_3H^+ species is also an s−p hybrid on the sulfur, and the p orbitals on the oxygens are normal to the plane. The antibonding in the associated SO_3H^+ fragment is reduced again due to the nonplanar geometry. The donor orbital in the SO_3H^+ adducts is again the d_{z^2} orbital of Pt with energies of −5.799 and −6.332 eV for Pt(II)−CH_3 and Pt(II)−Cl, respectively. The formation of the adduct with Pt(II)−CH_3 is again more favorable because of the higher energy of the donating d_{z^2} orbital. The SO_3H^+ fragment accepts electron charge from Pt of 0.64 and 0.7 in the dichloro and methyl complexes, respectively. Thus protonation of SO_3 enhances the transfer of electron density from Pt. However the transfer is still larger in the case of the methyl complex **C** compared to **A**.

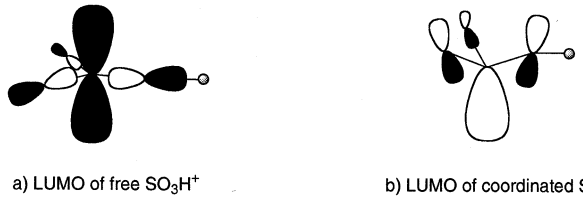

Figure 5. LUMO orbitals of SO_3H^+.

In the course of the complete oxidation reaction SO_3H^+ has to accept two electrons from Pt, to reduce the sulfur from oxidation state six to oxidation state four. Although the formation of compound 3 (Figure 3) seems much more favorable in the case of the Pt−CH_3 complex in absolute terms, and the transfer of electron density is greater, the calculated internal barrier is basically the same, around 34.6 kcal/mol for both systems. The energy profiles for the oxidation of the methyl and dichloro complexes are shown in Figure 6 as a function of the difference coordinate R(S−OH) − R(Pt−OH), where S−OH is the bond being broken and Pt−OH the bond being formed.

In the oxidation profile one can see for both oxidation processes a transition state followed by a shallow minimum and an additional increase in energy as the S−O bond is stretched further. The highest energy point (transition state) lies in different parts of the oxidation profile for the two complexes. For the platinum dichloro complex the highest energy point (TS-A) is after the minimum, whereas for the methyl complex (TS-B) it is before this minimum. The transition states corresponding to the highest energy points are indicated as compound 4 in Scheme 2, and their geometries are shown in Figure 7.

In the case of the methyl complex the bipyrimidine ligand is distorted with a dihedral angle of 15°, whereas

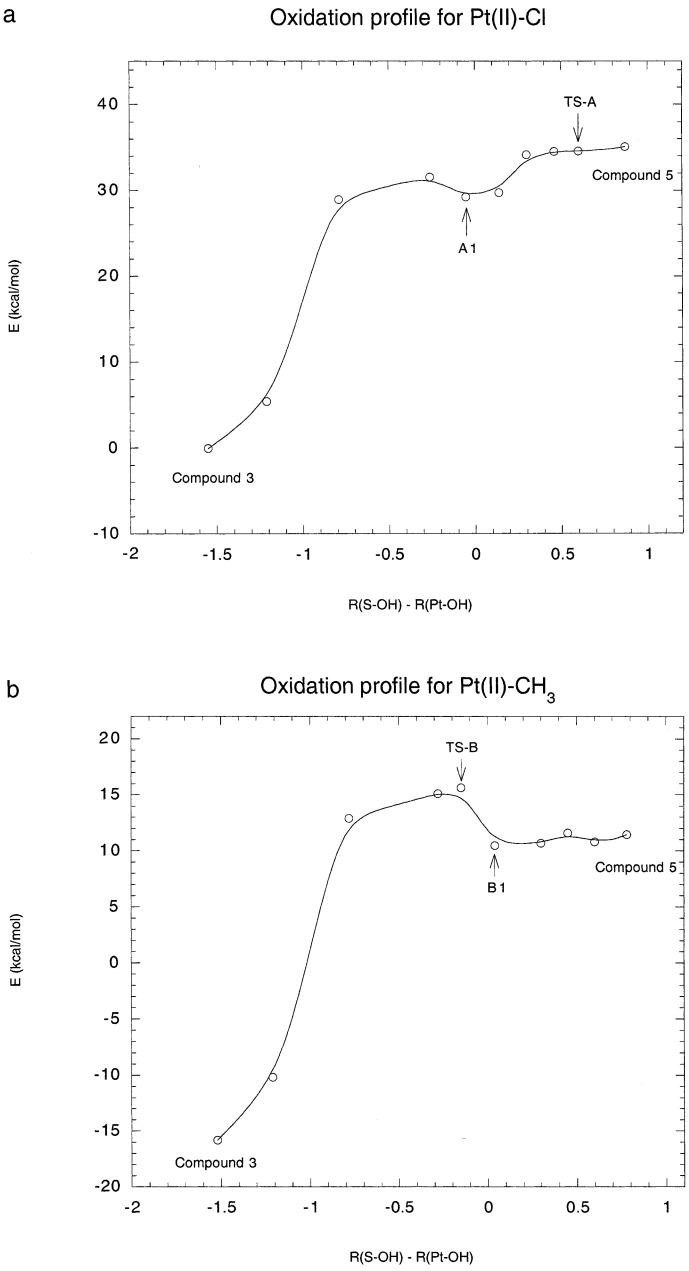

Figure 6. Energy profile for the linear transit compound 3 → 5 for (a) (bpym)$PtCl_2$ and (b) (bpym)$PtCH_3Cl$.

in the dichloro complex it always stays planar. The transition state for the dichloro complex (TS-A) has practically the same energy as the end product (compound 5 in Scheme 2), in which the S−O bond is already 2.86 Å, compared to 2.6 Å in the transition state. The barrier for the process is 34.4 kcal/mol in solution. To confirm the minimum in the profile, we did an unconstrained optimization of the structure from the linear transit (point A1), which yielded the exact same geometry (Figure 8a).

In the case of the platinum methyl complex the highest energy point (TS-B) is earlier on in the profile and corresponds to a barrier of 15.6 kcal/mol. After performing an unconstrained optimization on the minimum from the linear transit (B1) we also found this to be a stationary point (Figure 8b). Here, a further stretching of the S−O bond has almost no effect on the energy.

In the final steps of the oxidation there are again considerable differences in the energies of the species involving the methyl and dichloro complexes. The dissociation of SO_2 stabilizes the dichloro complex by 13.6 kcal/mol, while the same step leads to a destabilization of only 0.7 kcal/mol for the methyl complex.

The differences in the energies for the methyl and dichloro species along the oxidation path can be attributed to the greater electronegativity of Cl, which withdraws electrons from Pt to a larger extent than methyl does, and thus makes the electron transfer to SO_3H^+ harder. This is also reflected in an analysis of the molecular orbitals. Thus the donating orbital on the complexes is the $5d_{z^2}$ orbital of Pt, which is an antibonding orbital that is destabilized more by the methyl ligand than by chloride. The higher energy of the donor orbital in the methyl complex makes it easier to donate electron density to the oxidizing agent.

The oxidation of (bpym)$PtCH_3Cl$ is exothermic by 22.2 kcal/mol, while the oxidation of the catalyst itself is

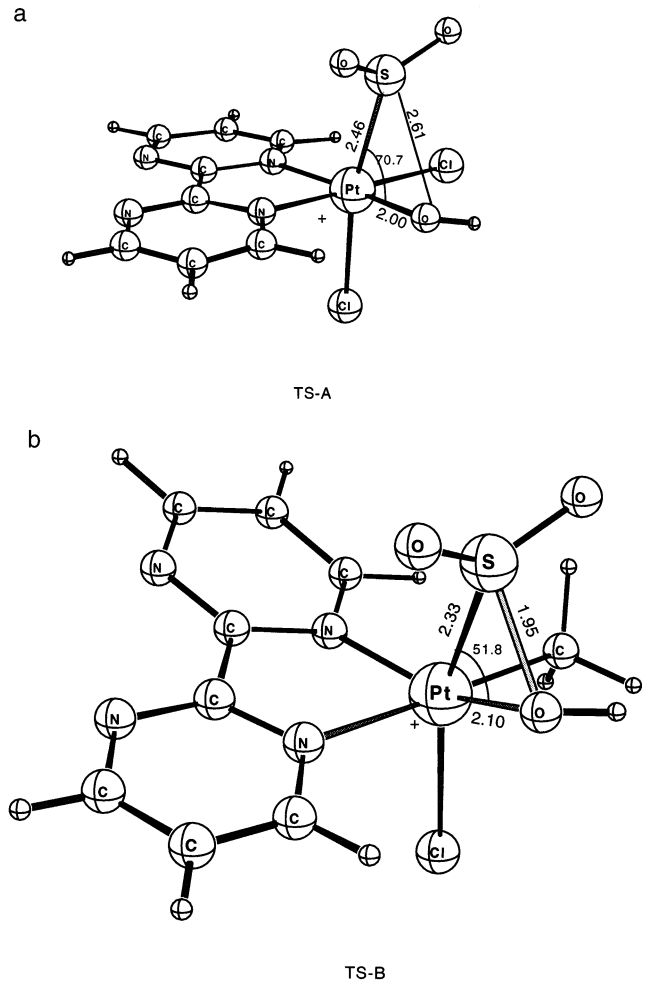

Figure 7. Transition states for the oxidation of (a) (bpym)$PtCl_2$ and (b) (bpym)$PtCH_3Cl$.

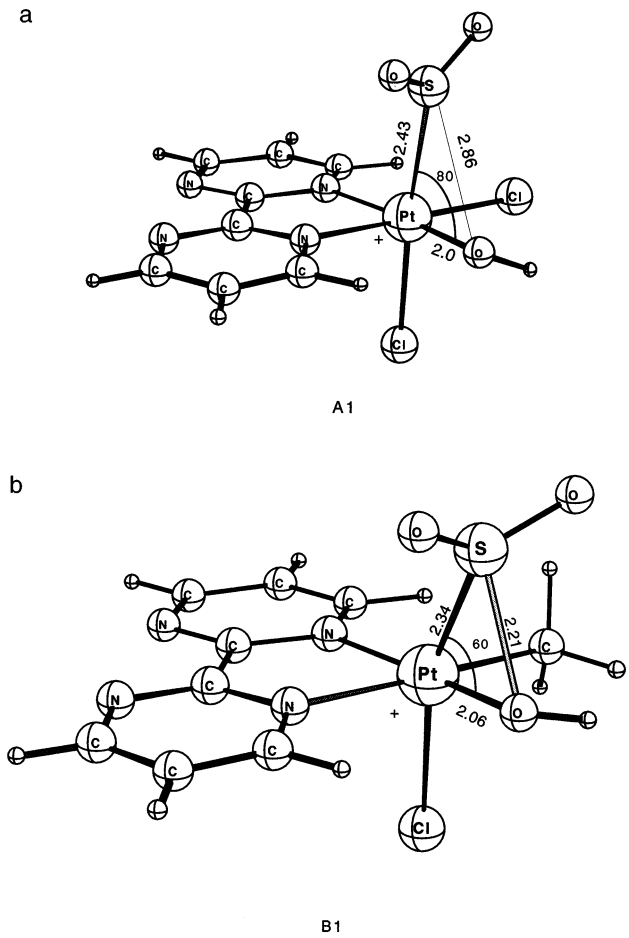

Figure 8. Local minimum structures in the linear transit compound 3 → 5 for (a) A1 and (b) B1.

endothermic by 8.3 kcal/mol. The overall barrier for the oxidation process is 35.1 kcal/mol for the catalyst (the dichloro complex) and 15.6 kcal/mol for the methyl complex, which rules out a two-step oxidation mechanism involving a Pt(IV) dichloro complex, and also confirms that the catalyst is stable toward SO_3 even under the harsh conditions applied in the Catalytica process.

Elimination. The final step in the Catalytica process is the reductive elimination of CH_3OSO_3H (see Scheme 1). The reductive elimination from the Pt(IV)−CH_3 complex **D** of Scheme 1 could proceed either by a concerted mechanism involving the CH_3 and OSO_3H groups bound to platinum or by a nucleophilic attack of an external OSO_3H^- group. For our system the mechanisms studied here are shown in Figure 9. The overall energy ΔH_6 for the process of reductive elimination,

$$Pt(IV)Cl(HSO_4)_2CH_3 \rightarrow Pt(II)Cl(HSO_4) + CH_3OSO_3H \quad (6)$$

is 1.9 kcal/mol. The internal elimination reaction is shown as mechanism A in Figure 9.

For the external elimination we have considered an S_N2 attack of a bisulfate group on a pentacoordinated Pt(IV) complex (**R1**, mechanism B), produced after dissociation of one bisulfate ligand, as well as an S_N2 attack of a bisulfate group on an octahedral complex with a concomitant release of another bisulfate ligand (mechanism C).

The barrier for the elimination process is not expected to be the rate-determining step in a Shilov system. As far as we know, this is the first computational study on a C−O reductive elimination from Pt(IV). The transition states for the reductive eliminations are shown in Figure 10.

The transition states were located with a linear transit calculation where the R(C−Pt) − R(C−O) bond length difference was kept frozen in the case of the S_N2 and dissociation/S_N2 attacks by an external nuclophile, whereas for the internal elimination the R(C−O) bond length was kept frozen.

A more unfavorable mechanism is the concerted elimination, with a barrier of 44 kcal/mol. The geometry of the transition state (Figure 10a) shows a strong distortion, while the Pt−C and Pt−O bonds that are supposed to be breaking are shorter than in the starting complex (Pt−C went from 2.04 to 1.96 Å; Pt−O, from 2.03 to 1.99 Å).

The most favorable pathway is the dissociation/S_N2 mechanism B of Figure 9, with a barrier of 16.1 kcal/mol. Here only one bond breaking takes place and the barrier is lower. The initial dissociation of a bisulfate ligand to produce the pentacoordinated Pt(IV) complex (**R1** in Figure 9) requires 1.7 kcal/mol in solution. The

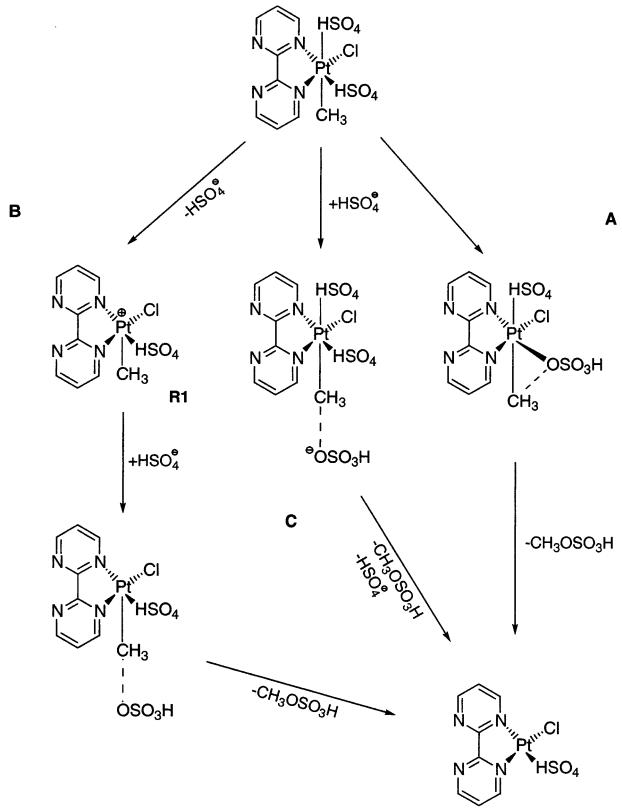

Figure 9. Reductive elimination mechanisms: (**A**) concerted, (**B**) dissociation/S_N2, (**C**) S_N2 with an external nucleophile.

bond lengths in the transition state (Figure 10b) are 2.44 and 1.99 Å for C−Pt and C−O, respectively. There is substantial experimental evidence that supports this dissociation/S_N2 mechanism for a Pt−phosphino system[8] and an S_N2 mechanism for the Shilov system.[9] However, for the Shilov system the experimental results cannot distinguish between the S_N2 and dissociation/S_N2 mechanisms.

In the case of the nuclophilic attack on an octahedral Pt(IV) complex, path C of Figure 9, we found that the transition state approaches that of the dissociation/S_N2 mechanism, path B of Figure 9, in that the SO_4H^- group trans to the methyl ligand had completely dissociated at the transition state.

Conclusion

The catalyst used in the Catalytica system is stable both to protonation at the nitrogens and to ligand exchange with bisulfate. The entering of methane into the first coordination sphere of Pt has a very high barrier, and the activation itself proceeds readily once the methane has entered. The preferred mechanism for the activation of CH_4 is oxidative addition. The oxidation of the Pt(II) complexes by SO_3 shows a high barrier for

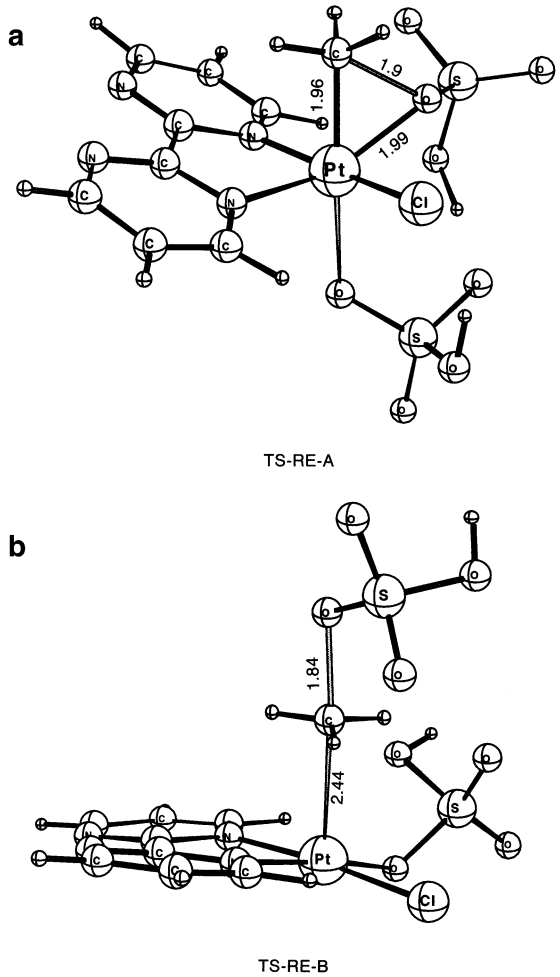

Figure 10. Transition states for the reductive elimination from Pt(IV)−CH_3: (a) mechanism **A**; (b) mechanism **B**.

the catalyst then the methyl complex, indicating that the oxidation of Pt(II)−CH_3 proceeds directly by the SO_3 oxidant and not by the prior formation of a Pt(IV)−dichloro complex. The mechanism for the oxidation involves protonation of SO_3, which is then stretched to form OH and SO_2 ligands at the platinum center.

After the completion of our computational work some new theoretical results on the Catalytica process became available.[10] Periana et al. suggest an oxidation mechanism where a double protonation of SO_3 takes place, which is then reduced by the Pt(II)−methyl complex to H_2SO_3. No calculated barriers were provided for this mechanism.

The reductive elimination proceeds by a dissociation/S_N2 mechanism in which a bisulfate ligand is dissociated from the oxidized six-coordinated Pt(IV)−methyl complex before nucleophilic attack of an external OSO_3H^- group on the CH_3 ligand.

Acknowledgment. This research was supported by funding from NSERC and the University of Calgary.

Supporting Information Available: The optimized geometries of structures discussed (Cartesian coordinates, in Å). This material is available free of charge via the Internet at http://pubs.acs.org.

OM020774J

(6) Procelewska, J.; Zahl, A.; van Eldik, R. *Dalton Discussion 4, Poster Abstracts, Inorganic Reaction Mechanisms: Insights into Chemical Challenges*; Kloster Banz: near Bamberg, Germany, Jan 10−13, 2002, p P26.

(7) Siegbahnn, Per E. M.; Crabtree, R. H. *J. Am. Chem. Soc.* **1996**, *118*, 4442.

(8) Williams, B. Scott; Goldberg, Karen I. *J. Am. Chem. Soc.* **2001**, *123*, 2576.

(9) Stahl, S. S.; Labinger, J. A.; Bercaw J. E. *Angew. Chem., Int. Ed.* **1998**, *37*, 2181 (review).

(10) Kua, J.; Xu, X.; Periana, R. A.; Goddard, W. A., III. *Organometallics* **2002**, *21*, 511.